Uncertainties in Episodic Ozone Modeling Stemming from Uncertainties in the Meteorological Fields

JHUMOOR BISWAS AND S. TRIVIKRAMA RAO

Department of Earth and Atmospheric Sciences, University at Albany, State University of New York, Albany, New York

(Manuscript received 8 October 1999, in final form 25 April 2000)

ABSTRACT

This paper examines the uncertainty associated with photochemical modeling using the Variable-Grid Urban Airshed Model (UAM-V) with two different prognostic meteorological models. The meteorological fields for ozone episodes that occurred during 17–20 June, 12–15 July, and 30 July–2 August in the summer of 1995 were derived from two meteorological models, the Regional Atmospheric Modeling System (RAMS) and the Fifth-Generation Pennsylvania State University–National Center for Atmospheric Research Mesoscale Model (MM5). The simulated ozone concentrations from the two photochemical modeling systems, namely, RAMS/UAM-V and MM5/UAM-V, are compared with each other and with ozone observations from several monitoring sites in the eastern United States. The overall results indicate that neither modeling system performs significantly better than the other in reproducing the observed ozone concentrations. The results reveal that there is a significant variability, about 20% at the 95% level of confidence, in the modeled 1-h ozone concentration maxima from one modeling system to the other for a given episode. The model-to-model variability in the simulated ozone levels is for most part attributable to the unsystematic type of errors. The directionality for emission controls (i.e., NO_x versus VOC sensitivity) is also evaluated with UAM-V using hypothetical emission reductions. The results reveal that not only the improvement in ozone but also the VOC-sensitive and NO_x-sensitive regimes are influenced by the differences in the meteorological fields. Both modeling systems indicate that a large portion of the eastern United States is NO_x limited, but there are model-to-model and episode-to-episode differences at individual grid cells regarding the efficacy of emission reductions.

1. Introduction

Increased levels of ozone in excess of the National Ambient Air Quality Standard for 1-h ozone concentrations are frequently observed over the northeastern United States. Surface ozone concentrations are controlled not only by in situ production, but also through pollutant transport, both of which are dictated by the prevailing meteorological conditions. Consequently, the issue of ozone problem is not limited to the urban area alone, and is instead a region-wide problem (Kumar and Russell 1996). The U.S. Environmental protection Agency (EPA) recently promulgated a new standard based on the daily maximum 8-h ozone concentrations (EPA 1997). Although the enforcement of the new standard is currently pending legal proceedings, it requires that the fourth highest 8-h ozone concentration in each year averaged over a consecutive 3-yr period be no greater than 0.08 ppm at any location. The shift from the 1-h standard to the 8-h standard has important implications for the ozone nonattainment issue. Because time and spatial scales are inherently connected in the ozone process (Rao et al. 1997), the 8-h standard may lead to a more widespread nonattainment problem (Chameides 1997).

The influence of meteorological conditions on ozone exceedance events in the northeastern United States has been investigated in several past studies (Pagnotti 1987; Gaza 1998; Zhang and Rao 1999; Zhang et al. 1998; Seaman and Michelson 2000). These studies have shown that, in addition to large-scale meteorological features, regional mesoscale structures play a vital role in creating conditions favorable for ozone accumulation. Given the sensitivity of ozone levels to the meteorological conditions, numerical modeling experiments are needed to provide insights into the dynamical processes responsible for ozone production and accumulation.

The EPA recommends that emission reductions needed to comply with the ozone standard be based on regional-scale photochemical model simulations of selected ozone episodes (EPA 1999). Photochemical models have been employed to simulate historical ozone episodes for evaluating emission control policies (Milford et al. 1989; Mathur et al. 1994; Roselle and Schere

Corresponding author address: Dr. S. T. Rao, Office of Science and Technology, New York State Department of Environmental Conservation, 50 Wolf Road, Albany, NY 12233-3259.
E-mail: strao@dec.state.ny.us

1995; OTAG 1997; EPA 1999). It has been shown that modeled ozone concentrations are sensitive to meteorological inputs and that emission control requirements based on one episode may be different from the emissions controls based on another episode (Sistla et al. 1996, 2001). Therefore, from a regulatory perspective, it is of interest to study the episode-to-episode fluctuations in model results stemming from varying meteorological inputs.

Meteorological fields for air quality simulations are usually derived from either observations or prognostic meteorological models. Because observational data are limited by low spatial and temporal resolutions, mesoscale forecasting models are increasingly being used to provide meteorological fields for air quality simulations. Modeled meteorological fields can provide a realistic representation of regional mesoscale features and reduce the uncertainty introduced by interpolation errors due to a sparse observational network. However, model-simulated meteorological fields are subject to uncertainty from sources such as model initialization, prescribed physical parameterizations, and data assimilation methods (Seaman and Michelson 2000; Shafran et al. 2000). Because a number of prognostic meteorological models are now being used in photochemical modeling analysis, a question that arises is whether there might be significant differences in the modeled ozone concentrations, and in the efficacy of an emission control strategy if different meteorological drivers are used for the same photochemical model. Therefore, the object of this study is to assess the uncertainties in modeled ozone concentrations due to the uncertainty in specifying the meteorological fields for the photochemical model. Also, we examine the directionality for emission controls (i.e., NO_x versus VOC sensitivity) as predicted by the photochemical model if two meteorological drivers are considered

The period of interest in this study is the summer of 1995, with particular emphasis on three ozone episodes that occurred during 17–20 June (June episode), 12–15 July (July episode), and 30 July–2 August (August episode). A description of the modeling systems and method of analysis is provided in section 2. The results from the analysis of the differences in the meteorological fields and predicted ozone concentrations are presented in section 3. Included in this section are the results from the hypothetical emission reduction scenarios and the directionality of controls (i.e., NO_x-focused versus VOC-focused reductions). The key findings of this study are summarized in section 4.

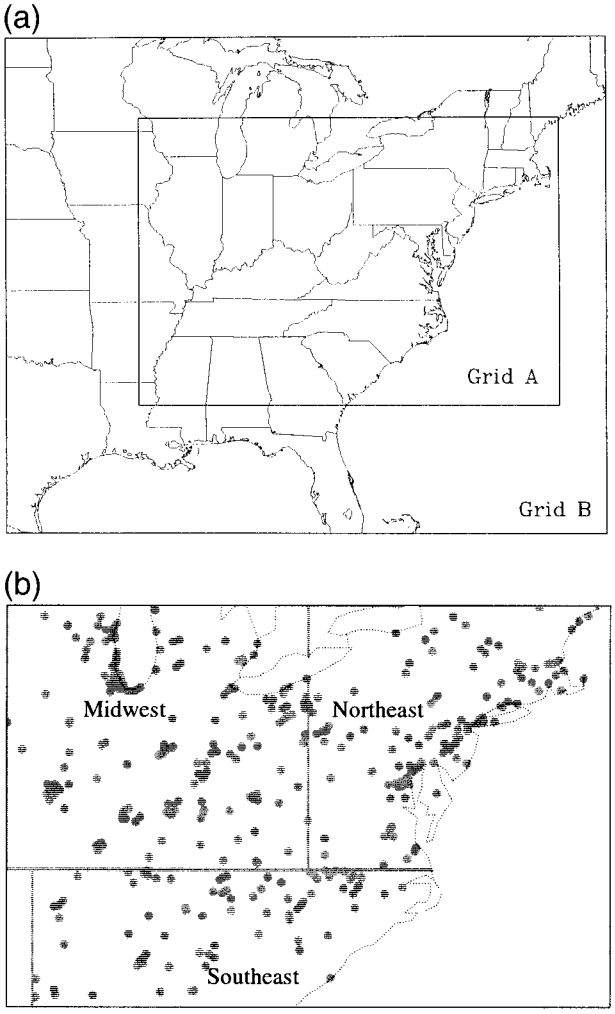

FIG. 1. (a) The UAM-V modeling domain and (b) the location of monitoring sites within the three subdomains in the fine-grid portion of UAM-V. The solid lines demarcate the three subregions: Northeast, Midwest, and Southeast.

2. Database and method of analysis

a. Photochemical modeling systems

The photochemical model used in this study is the three-dimensional grid-based Variable-Grid Urban Airshed Model (UAM-V), version 1.24 (fast chemistry solver), with the Carbon Bond Mechanism, version IV (Gery et al. 1988, 1989) and updated isoprene chemistry (SAI 1995). The UAM-V model has been used in the past for regulatory purposes (OTAG 1997). The two meteorological drivers commonly used for photochemical modeling applications are the Regional Atmospheric Modeling System (RAMS; Pielke and Ulisaz 1998) and the Fifth-Generation Pennsylvania State University–National Center for Atmospheric Research Mesoscale Model (MM5; Dudhia 1993).

UAM-V has been applied in the nested-grid mode (Fig. 1) with the inner fine grid A at 12-km horizontal gridcell dimensions extending from 92° to 69.5°W and from 32° to 44°N (137 columns by 110 rows) and a coarse grid B with 36-km grid cells, extending from 99° to 67°W and from 26° to 47°N (64 columns by 63 rows). The UAM-V model consists of 14 vertical layers extending from the surface up to 4 km. RAMS has 28

vertical layers over the fine-grid portion of the modeling domain, and MM5 has 25 vertical layers. Both meteorological drivers have nested grids with horizontal grid cell dimensions of 12, 36, and 108 km, with the outermost grid covering most of North America. The meteorological outputs from RAMS are in the polar stereographic projection system, and those of MM5 are in the Lambert conformal projection system. The meteorological outputs from RAMS and MM5 are made compatible with the UAM-V grid configuration by performing coordinate transformations and interpolations along the horizontal and vertical levels. Because the UAM-V domain along the vertical does not span the entire troposphere, vertical velocities are not constrained to be zero at the upper boundary. The mass exchange at the upper boundary is driven by the vertical velocity at the top, which is dynamically equivalent to the vertically averaged divergence. A pertinent issue that arises is the potential for mass inconsistencies in the final UAM-V ready meteorological fields as a result of the coordinate transformation and interpolation process. This problem is an inherent limitation of the discrete, grid-based modeling system wherein the photochemical and the meteorological models have different grid configurations.

Hourly meteorological data from 1 June to 31 August 1995 were simulated with RAMS version 3b (Lagouvardos et al. 1997) and MM5 (Zhang and Rao 1999) using four-dimensional data assimilation (4DDA). Although there are differences in the nudging procedures, both models used the same meteorological observations in data assimilation. The UAM-V simulations with two meteorological drivers have been carried out with the same emissions, boundary conditions, and initial conditions. Consequently, the differences in ozone simulations from the two modeling systems (hereinafter referred to as RAMS/UAM-V and MM5/UAM-V) are primarily attributable to the differences in the meteorological fields employed. Details on the differences in the prescribed processes in RAMS and MM5 can be found in Sistla et al. (2001).

The initial conditions for the modeling systems were set at background levels, and the model was allowed to spin up for three days as in Sistla et al. (2001). The boundary conditions for ozone at the top of the UAM-V model were obtained from daily available ozonesonde measurements. The emission inventory was derived using EPA's ''MOBILE 5'' (EPA 1998), a model for processing the mobile source emissions, and the Biogenic Emissions Inventory System, version 2 (Guenther et al. 1993; Geron et al. 1994) for biogenic emissions. Details regarding the preparation of emission inventories have been presented in Rao et al. (2000a). In addition to the base case simulation, the following scenarios with uniform emission reductions at all grid cells were also simulated:

- NO_x reduction by 25% and VOC reduction by 25% (n25v25),
- NO_x reduction by 25% and VOC reduction by 50% (n25v50), and
- NO_x reduction by 50% and VOC reduction by 25% (n50v25).

b. Observations

The observational data used in this study for both ozone and precursors are extracted from EPA's Aerometric Information Retrieval System (AIRS) database. For the analysis of the results requiring comparisons with observations, only model grid cells that contain or are adjacent to observational sites are chosen and modeled values are bilinearly interpolated to the monitoring site from the four cells surrounding the monitoring site as in Tesche et al. (1990). The locations of the observational sites used in this study are depicted in Fig. 1. The choice of these monitoring sites is based on the availability of continuous ozone data for the period of interest. Note that EPA's AIRS database consists of ozone monitoring primarily at urban-influenced sites.

c. Subdomains

To study region-to-region differences in model results and observations, the fine-grid domain of UAM-V is divided into the following three subdomains as shown in Fig. 1:

- Northeast subdomain (36.33°–44°N, 80.5°–69.5°W), which covers most of the northeastern urban corridor;
- Midwest subdomain (36.33°–44°N, 92°–80.5°W), which covers the Lake Michigan region; and
- Southeast subdomain (32°–36.33°N, 91°–69.5°W), which covers Atlanta and other urban regions in the Southeast.

d. Statistical measures

To obtain a perspective on the performance of the two models in simulating the observed ozone concentrations, we applied two statistical measures: 1) unpaired peak accuracy, and 2) absolute gross error, both expressed as a percentage. The former provides a measure of a model's ability to simulate the peak ozone concentrations, and the latter is a measure of the model's overall performance (Fox 1981). After Sistla et al. (1996), both sets of statistical calculations are performed on the hourly measured concentrations greater than or equal to 60 ppb and the corresponding model-simulated concentrations. The calculations are based on the measured and simulated values for 355 sites shown in Fig. 1b. The unpaired peak accuracy is expressed as

$$\frac{100(C_o - C_e)}{C_o}\%, \tag{1}$$

where C_o and C_e are the measured and modeled peak ozone concentrations, respectively. Note that C_o and C_e

may not necessarily be concurrent or collocated. Thus, this statistic is unpaired, both in space and time. The mean absolute normalized gross error is given by

$$\frac{100}{N}\sum_{i=1}^{N}\left|\frac{C_o(x_i, t) - C_e(x_i, t)}{C_o(x_i, t)}\right|, \quad (2)$$

where $C_o(x_i, t)$ and $C_e(x_i, t)$ are measured and modeled concentrations, respectively, at location i at any given time t, and N is the total number of monitoring locations.

The uncertainty in the modeled ozone concentrations is also examined by computing the mean-square error, systematic and unsystematic errors, and the range of variability as in Rao et al. (1985). The systematic error is a measure of the bias in a model, and the unsystematic error is a measure of the inherent variability in the results from the two models (Wilmott 1981). The unsystematic mean-square error (MSEU) and the systematic mean-square error (MSES) are computed using the following expressions (Rao et al. 1985):

$$\text{MSEU} = \frac{1}{N}\sum_{i=1}^{N}(P_i - \hat{P}_i)^2 \quad \text{and} \quad (3)$$

$$\text{MSES} = \frac{1}{N}\sum_{i=1}^{N}(\hat{P}_i - M_i)^2, \quad (4)$$

where $\hat{P} = a + bM_i$; a is the intercept, and b is the slope of the regression line; and P and M represent the two modeling systems, respectively.

e. Conventions

The following conventions are followed for the computations presented in this study:

- differences in the models' meteorological variables and in ozone levels are defined as (RAMS − MM5) and (RAMS/UAM-V − MM5/UAM-V);
- differences between the observed and modeled ozone levels are defined as (observed − RAMS/UAM-V) and (observed − MM5/UAM-V);
- percentage differences between the observed and modeled ozone levels are defined as 100 (observed − RAMS/UAM-V)/observed and 100(observed − MM5/UAM-V)/observed;
- percentage differences between model meteorological parameters and between ozone levels are defined as100(RAMS − MM5) and 100(RAMS/UAM-V − MM5/UAM-V)/RAMS/UAM-V; and
- the index of improvement of modeled ozone concentration as a result of the emission reduction is defined as

$$100\frac{(C_b - C_c)}{C_b}\%, \quad (5)$$

where C_b is the peak 1-h ozone in the base run, and C_c is the peak 1-h ozone in the control run at each grid point.

3. Results and discussions

a. Differences in meteorological parameters

Air pollution events are influenced by complex interactions between different processes such as vertical mixing, dilution, chemical production, and removal, which are affected by the prevailing meteorological conditions. Lagouvardos et al. (2000) and Sistla et al. (2001) have described the meteorological conditions associated with each of the three episodes of interest in this study. Detailed analysis of specific episodes have also been presented in Gaza (1998) and Seaman and Michelson (2000). Features common to the three ozone episodes are the slow eastward-moving ridge of high pressure at the 500-hPa level, the subtropical high over the Atlantic Ocean, and the Appalachian leeside trough, a mesoscale surface trough that is often associated with ozone episodes in the Northeast United States (Pagnotti 1987; Gaza 1998). Subsidence, near-stagnant surface flow and high temperatures associated with the high pressure system generally lead to the buildup of ground-level ozone concentrations. In addition, the enhancement of southwesterly winds as a result of the combined influence of the subtropical high over the Atlantic and the Appalachian leeside trough allow for the channeling of the pollutants along the northeastern urban corridor. The performance of mesoscale models during ozone episodes has been compared with observations in past studies (e.g., Seaman and Michelson 2000; Shafran et al. 2000). The performance of the RAMS and MM5 simulations used in this study have been examined by Hogrefe and Rao (2000) and Rao et al. (2000b), respectively. A detailed analysis of the differences in the meteorological fields obtained from the RAMS and MM5 is beyond the scope of this paper, but we present a few meteorological parameters to illustrate their influence on the ozone results from the two modeling configurations.

The differences in the peak daily surface temperature from RAMS and MM5 outputs, averaged over each episode and over all the 14 layers of the UAM-V, are presented in Fig. 2. Past studies (e.g., Alapaty et al. 1997; Shafran et al. 2000) have shown that differences in the thermal structure can arise from differences in the boundary layer parameterizations and upper boundary conditions in mesoscale models and, therefore, it is of interest to examine the differences in the temperature predictions of RAMS and MM5. Figure 2 shows that averaged daily maximum temperatures derived from RAMS are slightly higher than those of MM5. Over land, RAMS peak temperatures are warmer than MM5 by up to 2–3 K. The systematic difference in temperatures is seen at each of the 14 layers of the UAM-V (not shown). The differences in the daily maximum temperature fields persists during each episode, covering almost the entire land area of the fine-grid UAM-V domain. The difference in RAMS and MM5 temperatures stem from the differences in the boundary layer treat-

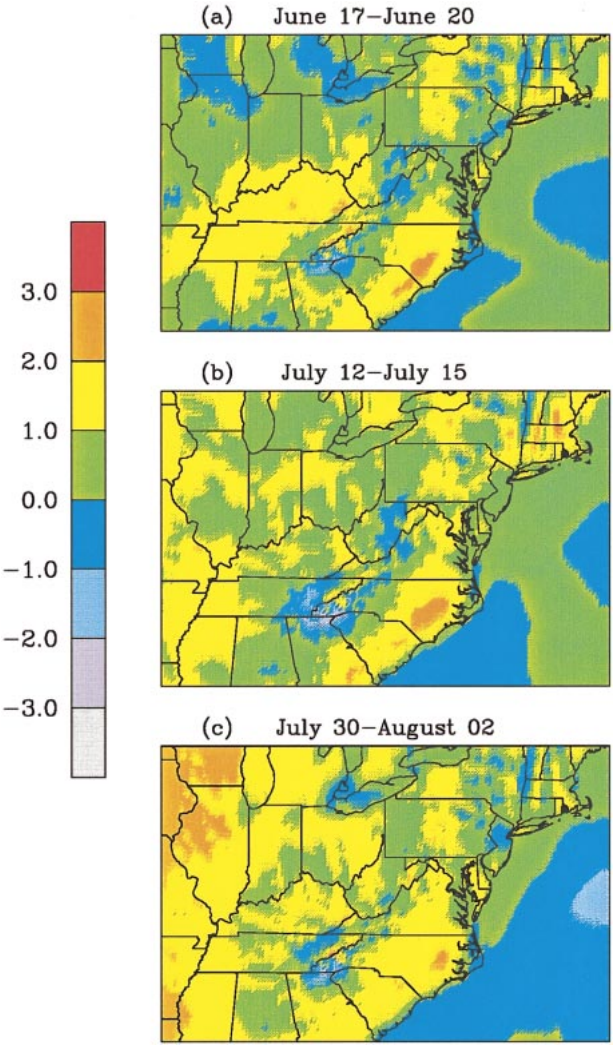

FIG. 2. Episode-averaged differences in the peak daily surface temperatures (°C) from RAMS and MM5 averaged over all 14 layers of UAM-V.

ment, soil and vegetation parameterizations, and radiation schemes in the two models. The differences may also be attributable to the differences in the data assimilation techniques used in the two models. The RAMS results were nudged to the European Centre for Medium-Range Weather Forecasts 6-hourly 4DDA outputs and 6-hourly surface observations, and the MM5 results were nudged to enhanced mesoscale analyses using soundings and 3-hourly surface observations from the National Centers for Environmental Prediction. The details of the difference in the two models have been described in Sistla et al. (2001). Sillman and Samson (1995) used a regional model (Sillman et al. 1990) to examine the effect of temperature on ozone results and showed that ozone concentration increases with temperature. However, in a study of the sensitivity of the Regional Oxidant Model (ROM) to prognostic and diagnostic meteorological fields, Alapaty et al. (1995) found that modeled ozone concentrations can differ by ± 90 ppb at individual grid cells even when there is a systematic bias in temperature and mixing heights.

Winds within the mixed layer play an important role in determining the amount of ozone accumulated in a region. The direction of prevailing winds also influences the ozone accumulation at individual locations. As noted earlier, the channeling of winds along the northeastern urban corridor through the combined influence of the subtropical high over the Atlantic and the Appalachian leeside trough can trap pollutants within this region, leading to high concentrations of ozone at the ground level. Thus, differences in the wind fields obtained from the two meteorological models can lead to a significant differences in ozone predictions from the photochemical model.

To illustrate, snapshots of winds from both modeling systems at three different hours are presented for one episode day (19 June) in Fig. 3. The surface winds in this subdomain during the morning hour are comparable in both models within the interior regions of the Northeast subdomain. However, over parts of Vermont, New Hampshire, and Massachusetts, winds from RAMS are higher. During the afternoon, winds from RAMS are higher by about 1.5–3 m s^{-1} within the northeastern urban corridor when compared with winds from MM5. Conversely, winds from MM5 are higher by about 1.5 m s^{-1} in portions of central New York and northern Pennsylvania. Differences in wind fields are also seen over Tennesee and Kentucky. Nighttime wind fields also show slight differences, with winds from RAMS being lower in the southern parts of the fine grid domain. Wind speeds from RAMS are also lower in northern New York, western Pennsylvania, Virginia, and North Carolina. Similar patterns are also seen during other days of the episodes (not shown). The strength and the location of the nocturnal jets in the Northeast show slight differences, but both models were able to resolve these features during the three ozone episodes (not shown).

The differences in the mixing heights in the two modeling systems are also examined. In the absence of an explicit formulation of mixing heights in the UAM-V, the vertical diffusivities obtained from RAMS and MM5 are used to estimate the mixing heights (Morris and Myers 1990). Thus, the differences in the mixing heights in the RAMS/UAM-V and MM5/UAM-V systems are attributable to the differences in the vertical diffusivity derived from RAMS and MM5. The vertical diffusivity in RAMS is computed from the vertical distribution of the turbulent kinetic energy (TKE), and the MM5 vertical diffusivity is diagnosed using an eddy-diffusion (K theory) method. Details regarding the computation of vertical diffusivity using these methods can be found in Pleim and Chang (1992) and Alapaty et al. (1997). It has been shown that vertical diffusivity computed using different methods can be significantly different and may potentially be a source of uncertainty in air quality modeling (Nowacki et al. 1996; Imhoff et al. 2000). Figure

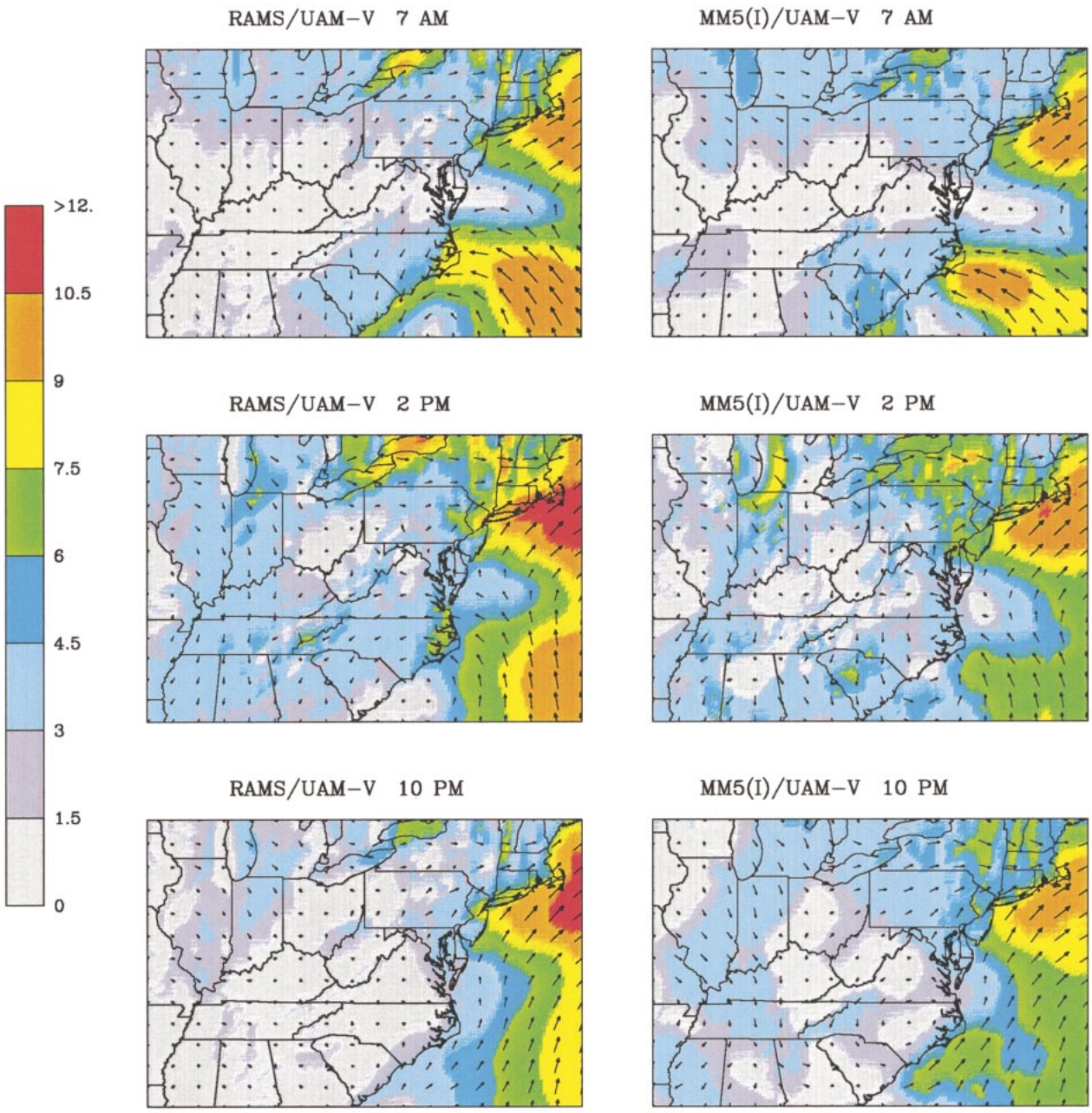

FIG. 3. Wind speeds at different hours from both models for 19 Jun.

4 depicts typical profiles of vertical diffusivity averaged over the morning hours from RAMS and MM5. The vertical diffusivity derived from MM5 is higher than RAMS in the lower layers. Imhoff et al. (2000) also find that the vertical diffusivity computed from RAMS using the TKE method yielded lower values when compared with other methods. The sensitivity of photochemical model results to the vertical diffusion parameterization has been examined by Nowacki et al. (1996) and Imhoff et al. (2000). Nowacki et al. (1996) found that reactive chemical species were more sensitive than ozone to vertical diffusion values, but Imhoff et al. (2000) showed that peak ozone concentrations were also influenced by vertical diffusion parameterization. To examine the influence of the mixing heights in the two modeling systems, the episode-averaged difference in morningtime (0600–1000) mixing heights is computed (Fig. 5). A systematic bias in the mixing heights can be seen in Fig. 5. The average morning mixing heights are higher in MM5 than in RAMS, a consequence of higher vertical diffusivity in MM5 (Fig. 4).

An additional parameter of interest is the morning

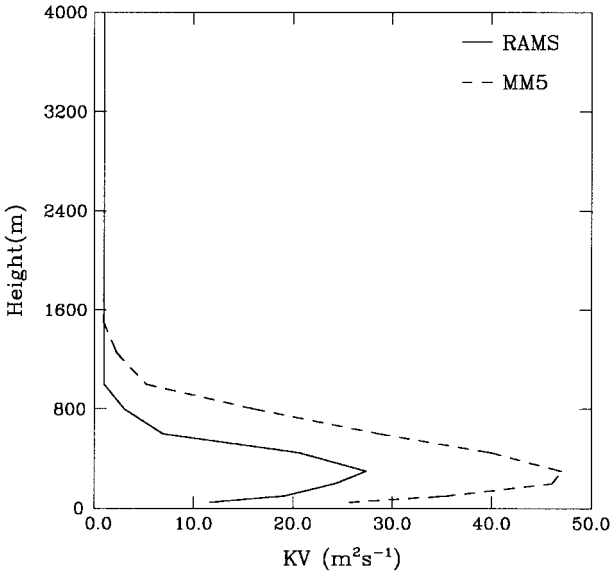

FIG. 4. Episode-averaged morningtime (0600–1000) profile of vertical diffusivity from RAMS and MM5.

ventilation coefficient, which is defined as the product of the mixing height and the surface wind speed. Rao et al. (2000b) used surface ozone data from 400 sites and found that the days with high ozone concentrations were associated with lower wind speeds, lower ventilation coefficients, and higher mixing heights than days with low ozone concentrations. Because the ventilation coefficient is a function of both wind speed and mixing height, it reflects the potential for vertical mixing and dilution of pollutants (Rao et al. 2000b). Polluted plumes of air, particularly in urban locations, are initially characterized by VOC-sensitive conditions (NRC 1999). Because chemical removal of NO_x proceeds at a faster rate than that of VOC, a transition from VOC- to NO_x-sensitive conditions occurs as the NO_x is processed and removed from the polluted air. However, the shift from VOC sensitivity to NO_x sensitivity is influenced by the rate of dilution of the polluted air. Under stagnant conditions, the amount of NO_x removed from the air may not be sufficient, consequently delaying the transition to NO_x sensitivity (NRC 1999). On the other hand, strong horizontal winds and vertical mixing of the air enhance the rate of removal of NO_x from the polluted plume and establish NO_x-sensitive conditions. Thus, lower ventilation coefficients imply near-stagnant conditions wherein an aging plume of polluted air remains under VOC sensitivity, while higher ventilation coefficients indicate rapid dilution of the polluted air, leading to NO_x-sensitive conditions. Typically, early mornings are associated with lower mixing depths and fresh emissions from automobiles, and the extent of mixing and dilution of polluted morning air determines peak ozone concentrations in the afternoon hours. It should be noted that morningtime ventilation coefficient includes the effect of both mixing and dilution and may play an important role in influencing ozone concentrations even during multiday regional-scale episodes.

In both modeling systems, the Northeast, coastal Southeast, and regions around the Great Lakes are associated with higher values of ventilation coefficients while lower values of ventilation coefficients are found in the Midwest (not shown). The general pattern of ventilation coefficients in the two modeling systems appears to be similar, but there are significant quantitative differences. To illustrate this point, the percentage difference in the episode-averaged morningtime (0600–1000) ventilation coefficients from the two models is presented in Fig. 6. Interior regions of the Northeast, including most of central and western New York and Pennsylvania, are associated with lower ventilation coefficients in RAMS/UAM-V system during each episode. Lower ventilation coefficients in the RAMS/UAM-V system are also found over Illinois, Missouri, and Wisconsin during the first two episodes. Another consistent feature that can be seen is that ventilation coefficients in the RAMS/UAM-V system are higher than the same in the MM5/UAM-V system (by up to 40%) over parts of Massachusetts, New Hampshire, and Vermont. These regions are also associated with higher winds speeds in RAMS/UAM-V (not shown). Higher values in the RAMS/UAM-V system are also seen over parts of Virginia during the 17–20 June and the 30 July–2 August episodes. During the latter episode, the higher ventilation coefficients from RAMS extend into Pennsylvania. It is seen that the differences in ventilation coefficient show significant episode-to-episode changes, indicating the influence of the winds in determining the ventilation coefficient differences during one episode and that of the mixing heights during another.

b. Model assessment

We use both 1-h and 8-h peak ozone concentrations from model results and observations for evaluating the model performance. The daily maxima of 1-h and 8-h ozone concentrations are more appropriate for comparison with observation than the hourly ozone values, because hour-to-hour variations in the hourly concentrations reflect high-frequency fluctuations (Hogrefe et al. 2000). Also, diurnal cycles inherently present in the hourly observed and modeled values lead to a greater correlation between them and may lead to incorrect interpretation of the model performance (Biswas and Rao 1999). The use of only the daily maxima instead of hourly values indeed reduces the number of data points available for analysis. However, our ability to characterize the behavior of the modeling systems over space is not overly compromised, despite the spatial correlation among the data, because of the large sample size. In the following sections, we discuss the performance of the two modeling systems, RAMS/UAM-V and

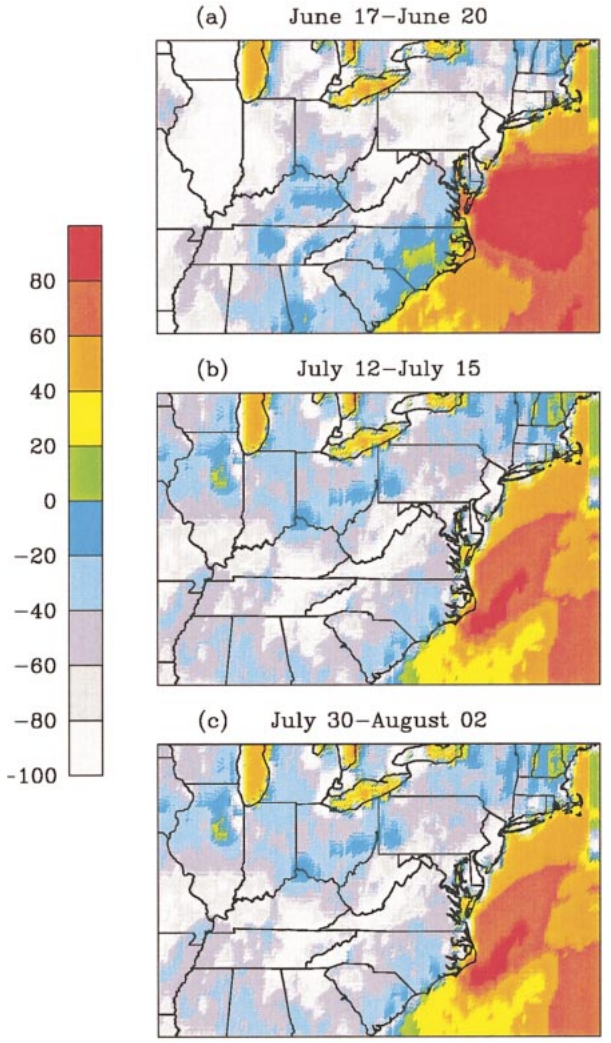

FIG. 5. Percent difference in episode-averaged morningtime (0600–1000) mixing heights from RAMS and MM5.

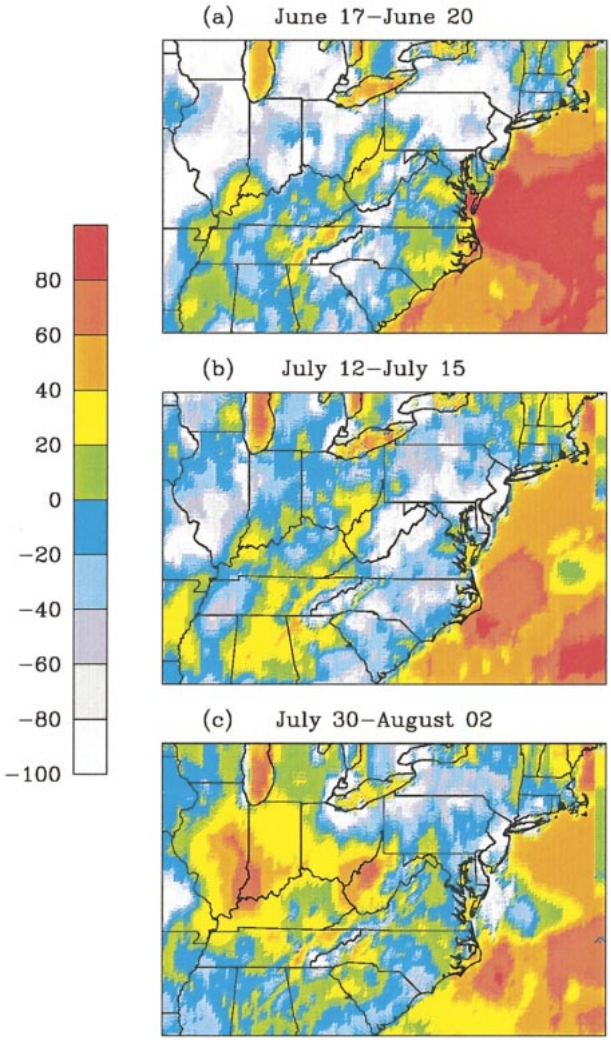

FIG. 6. Percent difference in episode-averaged morningtime (0600–1000) ventilation coefficients from RAMS and MM5.

MM5/UAM-V, focusing on the variability of ozone predictions.

1) MODEL EVALUATION: COMPARISON BETWEEN MEASURED AND SIMULATED OZONE CONCENTRATIONS

The performance of each modeling system is examined using the measured concentrations of ozone at the selected sites based on the statistical measures recommended by EPA (1991). We assess the ability of each modeling system to reproduce the observed ozone levels at individual sites and spatial patterns of modeled ozone concentrations within the fine-grid domain of the UAM-V.

(i) Unpaired peak accuracy and absolute mean gross error

The results from these metrics for each day of the three episodes are summarized in Table 1. The RAMS/UAM-V system underpredicts ozone levels on most days while the MM5/UAM-V underpredicts on some days and overpredicts on other days. Thus, the RAMS/UAM-V system has a consistent bias on most days, while the MM5/UAM-V system fluctuates on either side of the measured values. A comparison of the unpaired peak accuracy values also suggests that the MM5/UAM-V system simulates higher ozone values than does the RAMS/UAM-V system. As expected, the results from the unpaired peak accuracy calculations show a considerable change if we were to include additional sites or exclude some of the existing sites, illustrating the problem with this metric.

The absolute mean gross error, being an average mea-

TABLE 1. Unpaired peak accuracy and absolute mean gross error, both expressed in percent, for each day of the three episodes for ozone concentrations simulated by RAMS/UAM-V and MM5/UAM-V.

	Unpaired peak accuracy		Absolute mean gross error	
	RAMS/ UAM-V	MM5/ UAM-V	RAMS/ UAM-V	MM5/ UAM-V
17 Jun	28.3	12.8	18.4	17.2
18 Jun	23.1	10.9	18.6	18.4
19 Jun	19.4	9.8	19.4	21.4
20 Jun	10.8	4.0	19.9	21.1
12 Jul	8.6	−3.6	20.0	20.9
13 Jul	8.2	−8.8	18.4	22.2
14 Jul	9.1	7.8	20.4	21.1
15 Jul	4.1	13.8	20.8	24.1
30 Jul	−4.0	−0.6	20.6	21.9
31 Jul	8.7	−5.4	21.4	22.8
1 Aug	16.3	7.7	19.4	23.3
2 Aug	1.5	−20.0	21.7	27.5

sure of the departures from the observed values and also being paired in space, is a relatively more stable measure of model errors. The results in Table 1 indicate that almost all values of this statistic are below 25% for both modeling systems, and, thus, are well within EPA's criteria for an acceptable model performance (EPA 1991). We also see that both models perform comparably, though the errors from MM5/UAM-V are slightly higher than those of RAMS/UAM-V.

(ii) Comparison of 1-h peak modeled and measured ozone

The regionwide performance of both modeling systems is assessed from the spatial pattern of the differences between the modeled and measured ozone concentrations. The percentage differences between the observed and modeled 1-h maximum ozone concentrations for each modeling systems are presented in Fig. 7. A brief discussion for each episode, based on the results depicted in Fig. 7, is given below.

For the June episode, from the spatial distributions of the percentage differences in episode-averaged 1-h daily maximum ozone, (Figs. 7a,d), it is evident that both models underpredict the observed peak ozone concentrations. There is an underprediction of peak ozone concentrations at about 80% of sites in the RAMS/UAM-V simulation and 66% in the MM5/UAM-V simulation. However, at a majority of sites, both models simulate ozone levels to within 20% of the observed peak ozone concentrations. These results reveal that both models are able to reproduce the observed spatial pattern of peak ozone concentrations despite a bias toward underprediction.

A feature common to both models is the underprediction of ozone in the northeastern urban corridor (Figs. 7a,d). In particular, the RAMS/UAM-V system appears to model lower peak ozone values than MM5/UAM-V does throughout the corridor extending from northern Virginia to Long Island. The presence of a few sites in the MM5/UAM-V system within the northeastern urban corridor that show higher-than-observed ozone levels may be linked to the lower afternoon winds in the model (Fig. 3). In the Midwest subdomain, the models are closer to the observed values. Sites in the Southeast show mixed results. The RAMS/UAM-V system underpredicts by up to 20% while the MM5/UAM-V system overpredicts peak ozone values at by about 20% of the observed values at sites around Atlanta. The spatial pattern of episode-averaged 8-h peak ozone concentrations is similar to the 1-h peak ozone values, though the 8-h peak ozone values from the MM5/UAM-V system show a greater departure from the observations than do those from the RAMS/UAM-V system (not shown).

The results for the July-episode daily maximum 1-h ozone (Figs. 7b,e), when contrasted with the June episode, illustrate the episode-to-episode variability in the performance of the two modeling systems. A prominent departure from the June episode can be seen clearly in the distribution of the percentage difference values (Figs. 7b,e). Over the entire domain, there appears to be almost an equal split in the number of sites that have under- and overprediction of ozone concentration. The bias toward underprediction in the two models along the northeastern urban corridor is not as prominent in this episode as it was in the June episode.

The MM5/UAM-V system has a greater percentage of sites for which there is an overprediction of the observed daily maximum 1-h ozone (Figs. 7b,e). At several sites in the RAMS/UAM-V simulations, there are significant differences from the June episode; for example, in the regions west of Lake Michigan, the RAMS/UAM-V system overpredicts ozone concentrations by about 20% where it had underpredicted ozone concentrations during the June episode. At a few sites in the Southeast, RAMS/UAM-V underpredicts ozone concentrations by 20%–40% whereas the MM5/UAM-V system underpredicts the concentrations by less than 20% (consistent with the higher ventilation coefficients in the RAMS/UAM-V system in parts of the Southeast).

Another feature of interest in the model simulations for this episode is the increased number of sites where the modeled values are significantly higher (20% or greater) than the observed peak ozone concentrations. For instance, at sites near Nashville and along the western border of Kentucky, the modeled ozone values are larger than 20% of the observed peak ozone values. The MM5/UAM-V system models higher ozone concentrations than the RAMS/UAM-V system at a large number of sites. For this episode, both models show a poorer performance for the 8-h peak ozone than for 1-h peak ozone (not shown).

For the August episode, the results from the percentage-difference calculations for the third episode are shown in Figs. 7c,f for 1-h ozone. The overall performance of the models for this episode is worse than in

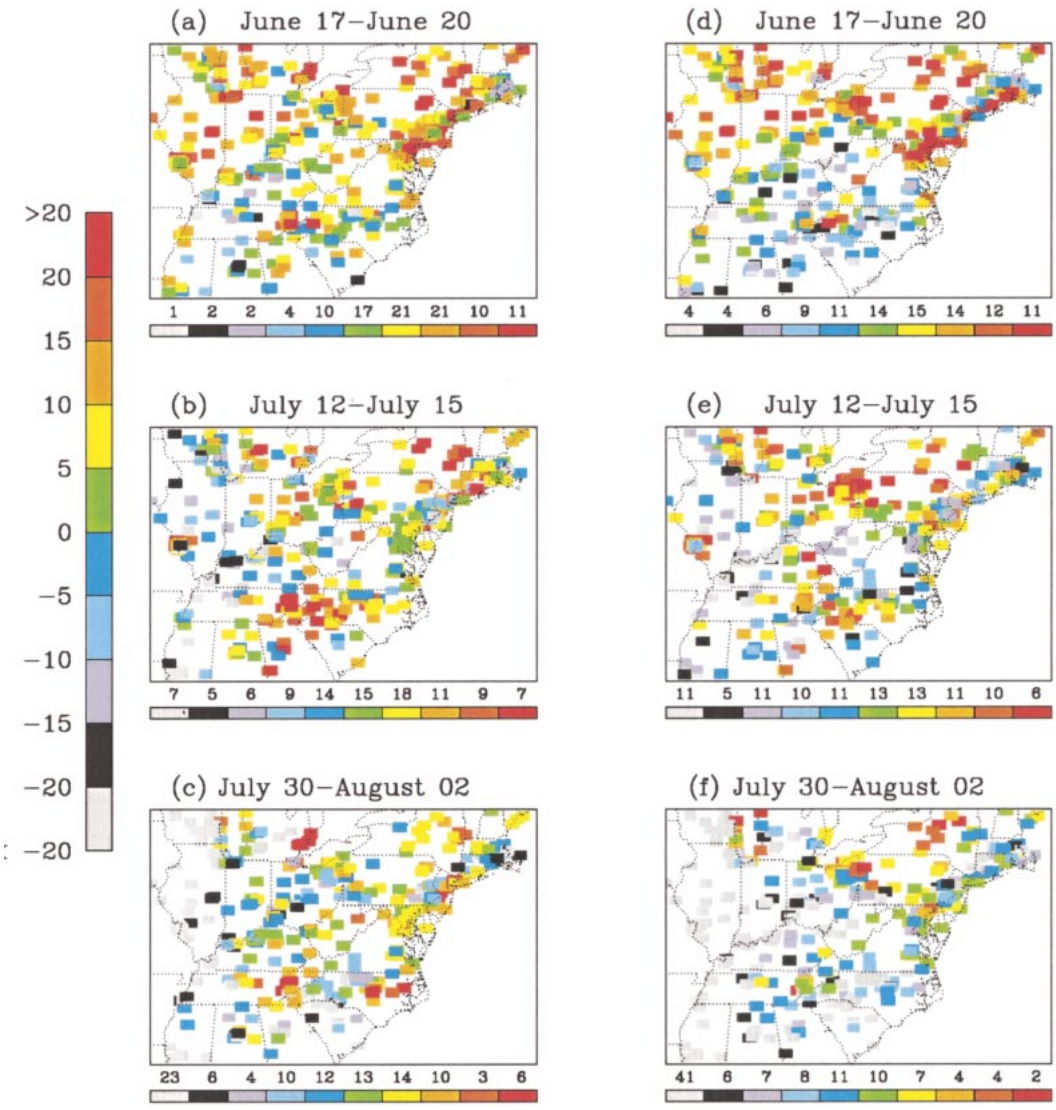

FIG. 7. Percent difference between the observed and modeled episode-averaged daily maximum 1-h ozone from (a)–(c) RAMS/UAM-V from (d)–(f) MM5/UAM-V. Numbers above the individual label bars denote the percent of sites that fall within each plotting interval. The common plotting scale is depicted by the large label bar.

the previous two episodes. Both models overestimate the peak ozone levels at many locations; the number of such sites is greater in MM5/UAM-V than in RAMS/UAM-V. The results for the 1-h peak ozone values (Figs. 7c,f) highlight the differences in the performance of the two models. The MM5/UAM-V system overpredicts the observed peak ozone levels at almost all the sites in the northeastern urban corridor, a significant change from the other episodes. On the other hand, the RAMS/UAM-V system underestimates the peak ozone levels in the urban corridor. As discussed earlier, the difference between the two models in these regions is related to the differences in the winds and ventilation coefficients in the two models. The MM5/UAM-V system has weaker winds along most of the urban corridor than RAMS/UAM-V, leading to greater amount of ozone accumulation in MM5/UAM-V. Ozone results in the Midwest are significantly higher than the observed values. At some locations, such as the Lake Michigan region, the modeled ozone values are in excess of 40% of the observed values. A similar pattern is evident for the 8-h peak ozone values (not shown).

(iii) Regionwide performance of the models

As noted earlier, we divided the modeling domain into three subdomains. (Fig. 1) to identify patterns in ozone results that might vary from one region to the other. To gain further insight into the sensitivity of the photochemical model to the differing meteorological drivers, the modeled daily peak ozone values are plotted against the measured values at the monitoring stations.

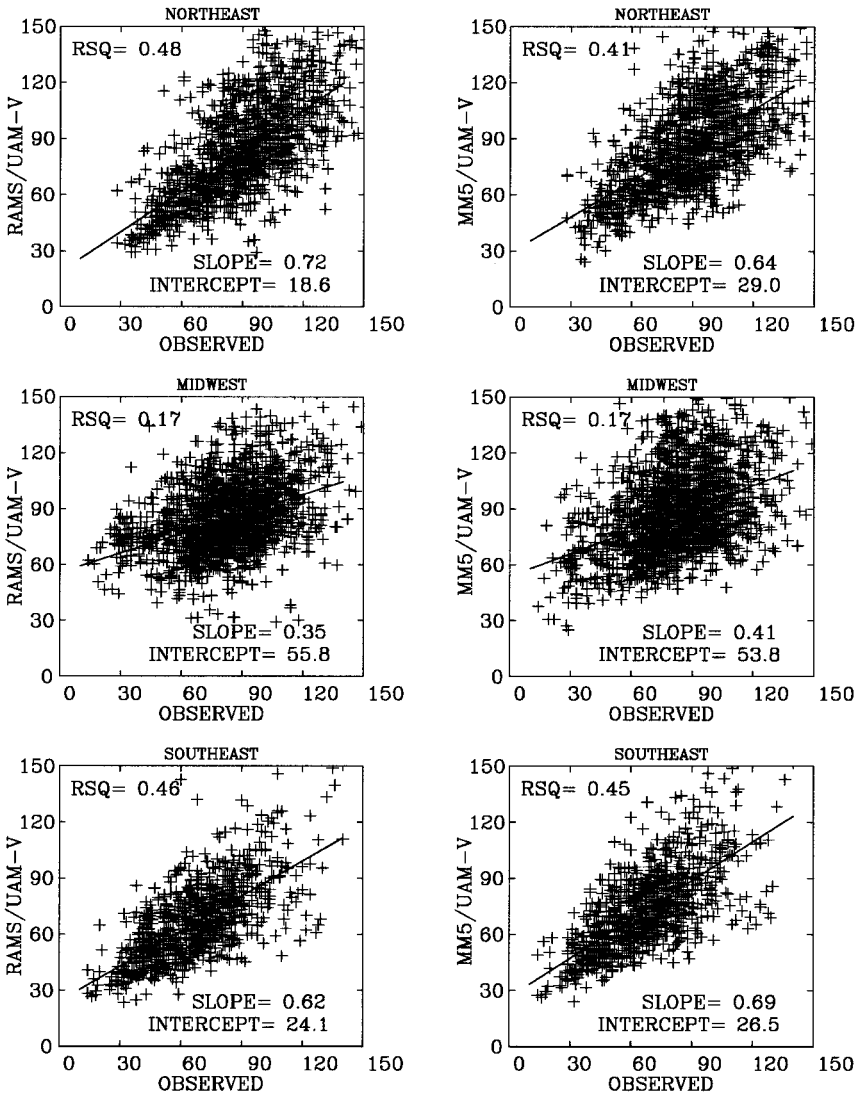

FIG. 8. Scatterplots of the observed and modeled (left: RAMS/UAMV; right: MM5/UAM-V) 1-h peak ozone for all the days of the three episodes for the (top) Northeast, (middle) Midwest, and (bottom) Southeast subdomains.

Each of the three episodes is considered so that the episode-to-episode differences may also be discerned.

The simulated daily maximum ozone for all days of the three episodes is plotted against the observed peak ozone concentrations for each subregion in Fig. 8. The straight line in each panel depicts the best linear fit obtained from the pairs of ozone values. The models fare comparably in each subregion. The values of the coefficient of determination (square of the correlation coefficient, RSQ) indicate that the models are able to explain approximately 50% of the variability in the observations over the Northeast and Southeast subdomains. Over all the episodes, the Northeast and Southeast regions have the best correlations while the Midwest has the lowest correlation. From Fig. 7, we see that the modeling systems generally overpredict concentrations in the lower range and underpredict in the higher range of ozone concentrations. This is more so in the case of MM5/UAM-V than in RAMS/UAM-V. The correlation results must be interpreted cautiously because the data are not, in a strict sense, statistically independent in time and space.

2) MODEL-TO-MODEL COMPARISON

The simulated ozone concentrations from the two modeling systems are compared with the aim of assessing the uncertainty in the results of the photochemical model stemming from differences in the sources for meteorological input variables. First, we examine the differences in the spatial pattern of ozone concentrations produced by the two modeling systems. Using the daily

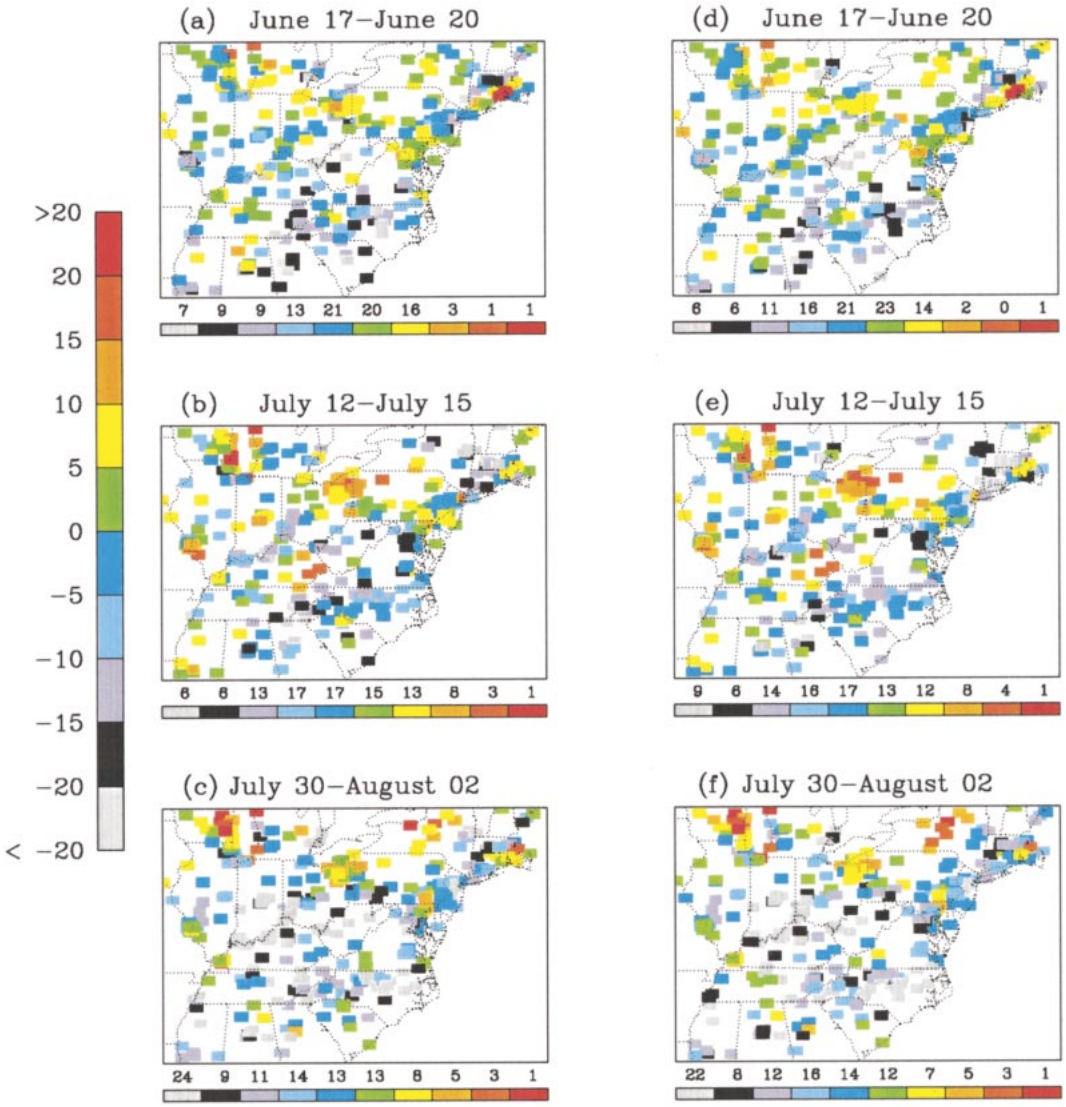

FIG. 9. Percent difference of simulated episode-averaged daily maximum (a)–(c) 1-h ozone and (d)–(f) 8-h ozone for each of the three episodes. Numbers above the individual label bars denote the percent of sites that fall within each plotting interval. The common plotting scale is depicted by the large label bar.

maxima of 1-h and 8-h ozone concentrations for a given episode, we computed the episode-averaged 1-h and 8-h ozone concentrations at all locations. This process eliminates the day-to-day variation within an episode and is useful in obtaining a general sense of the difference between the two models for a given episode. As mentioned earlier, these calculations are performed for the model grid cells corresponding to the monitoring sites shown in Fig. 1. The percentage differences, between the two modeling systems, for the episode-averaged 1-h and 8-h peak ozone concentrations are displayed in Fig. 9. The figures are plotted on the same scale to aid the quantification of the differences, and the percent of sites that fall within each interval is provided above the individual label bars.

It is evident that the spatial patterns of differences in the peak ozone concentrations from the two modeling systems vary from episode to episode (Fig. 9). However, we find that the results in the modeled 1-h and 8-h ozone levels at most sites (e.g., 92% of all sites during the June episode) are within 20% of each other. The largest discrepancy between the two models is seen for the August episode for which the MM5/UAM-V simulated ozone levels are in excess of 20% of the results of the RAMS/UAM-V system for more sites than in the previous two episodes (24% of all sites for the 1-h ozone maxima and 22% of all sites for the 8-h ozone maxima). These sites are mostly in the interior of the Midwest and Southeast subdomains. Among features of interest, peak ozone in the northeastern urban corridor is consistently lower in RAMS/UAM-V than in MM5/UAM-V. Also, the RAMS/UAM-V system gives higher

values in regions west of Lake Michigan and some sites in eastern Pennsylvania during each episode. These features are consistent with our findings regarding the wind speeds and ventilation coefficients in these regions. The regions along the northeastern urban corridor are associated with higher afternoon winds, leading to greater mixing and dilution of ozone in RAMS/UAM-V. Conversely, the higher ozone levels along the Great Lakes are attributable, in part, to the lower wind speeds and ventilation coefficients in RAMS/UAM-V. Ozone concentrations in the Southeast region are consistently lower in RAMS/UAM-V than in MM5/UAM-V. This result may also be related to the higher wind speeds in the RAMS/UAM-V system, which leads to greater dilution of the polluted air.

The influence of the consistent bias in the peak temperature over the entire modeling domain (see Fig. 2) on ozone simulations made by the two modeling systems is less evident. The effects of the bias in temperature might have been offset by the spatial variability found in the winds and ventilation coefficients. Similar results were also found by Alapaty et al. (1995) when they used prognostic and diagnostic meteorological inputs for the ROM simulations. The ventilation coefficient, being function of both mixing height and wind speed, exerts a greater influence on ozone buildup within any region.

The model-to-model differences in ozone results are also presented in the form of the distribution of the differences in the modeled daily 1-h ozone maxima (Fig. 10). The MM5/UAM-V results are, in general, higher than those of RAMS/UAM-V (the mean of each distribution is negative), consistent with earlier results. Also, the distributions are nearly symmetric around the mean, the exception being the distribution for the August episode. These distribution plots are useful in characterizing the variability associated with ozone modeling due to uncertainties in meteorological modeling. Assuming the normal distribution for the differences, the approximate 95% confidence interval for the mean difference is about $\pm$16 ppb for the June episode, $\pm$20 ppb for the July episode, and $\pm$24 ppb for the August episode. When data from all three episodes are combined, the approximate 95% confidence interval for the mean difference is about $\pm$20 ppb (Fig. 10d). In other words, the model-to-model differences in simulating ozone concentrations can vary as much as 20 ppb because of the uncertainties in the specification of the meteorological fields.

Table 2 shows the MSES and the MSEU computed from the 1-h maximum ozone values. To assess the spatial differences in different subdomains, the results are presented for the Northeast, Midwest, and Southeast subdomains described in Fig. 1. The Northeast and the Midwest subdomains are characterized by model differences that are predominantly unsystematic errors (Table 2). However, in the Southeast, the MSE is composed mostly of systematic errors. The dominance of the unsystematic errors in the Northeast and Midwest subdomains indicates the inherent uncertainty in the model results in these subdomains, while higher systematic error in the Southeast is a reflection of a bias in the models that might be corrected to improve the results. The June episode is associated with the lowest values of rmse in each subdomain, and the August episode is associated with the highest values. The larger rmse found for the August episode is related to the greater discrepancy in the meteorological inputs for this episode as compared with the June and July episodes.

The range of variability, defined in terms of the 95% confidence interval for the difference in the modeled ozone peak concentrations, is also determined for the selected sites. The results, expressed as a percent of the mean simulated ozone from the two models, also are presented for each episode in Table 2. The Northeast and Midwest subdomains show a higher model-to-model variability when compared with the Southeast. Most values are around 20%, but the range of variability can be as high as 34% (for the Midwest for the July episode from Table 2). This result, together with the finding that a large percentage of the errors in the Northeast and Midwest subdomains are of unsystematic type, reveals the magnitude of uncertainty in simulating absolute ozone levels in the eastern United States.

c. VOC limitation versus NO_x limitation

Ozone formation is a nonlinear process involving chemical reactions among volatile organic compounds (VOCs) and carbon monoxide in the presence of nitrogen oxides (NO_x) and sunlight (Lu and Chang 1998). The VOC limitation and NO_x limitation characteristic of an air parcel vary dynamically with transport, dispersion, dilution, and photochemical aging. Because photochemical models are being used in a regulatory setting, it is important to assess the variability in the response of the modeling systems to various emission control strategies.

EFFICACY OF EMISSION REDUCTIONS

We compute the index of improvement for the n25v50 and n50v25 control runs relative to the base case run n00v00, averaged over all the three episodes. The results from both modeling systems, presented in Fig. 11, suggest that both models show a greater sensitivity to reductions in NO_x emissions than in VOC emissions. A 50% reduction in NO_x and 25% reduction in VOC emissions leads to a decrease in episodes-averaged peak ozone levels by 15% or higher over most of the domain (Figs. 11c,d), and a 50% decrease in VOC and 25% reduction in NOx emissions yields 5%–15% decreases in ozone levels (Figs. 11a,b). Although the results from both models are similar, there are differences at individual grid cells; for example, in the Northeast region, RAMS/UAM-V indicates a smaller ozone benefit from NO_x reductions when compared with MM5/UAM-V.

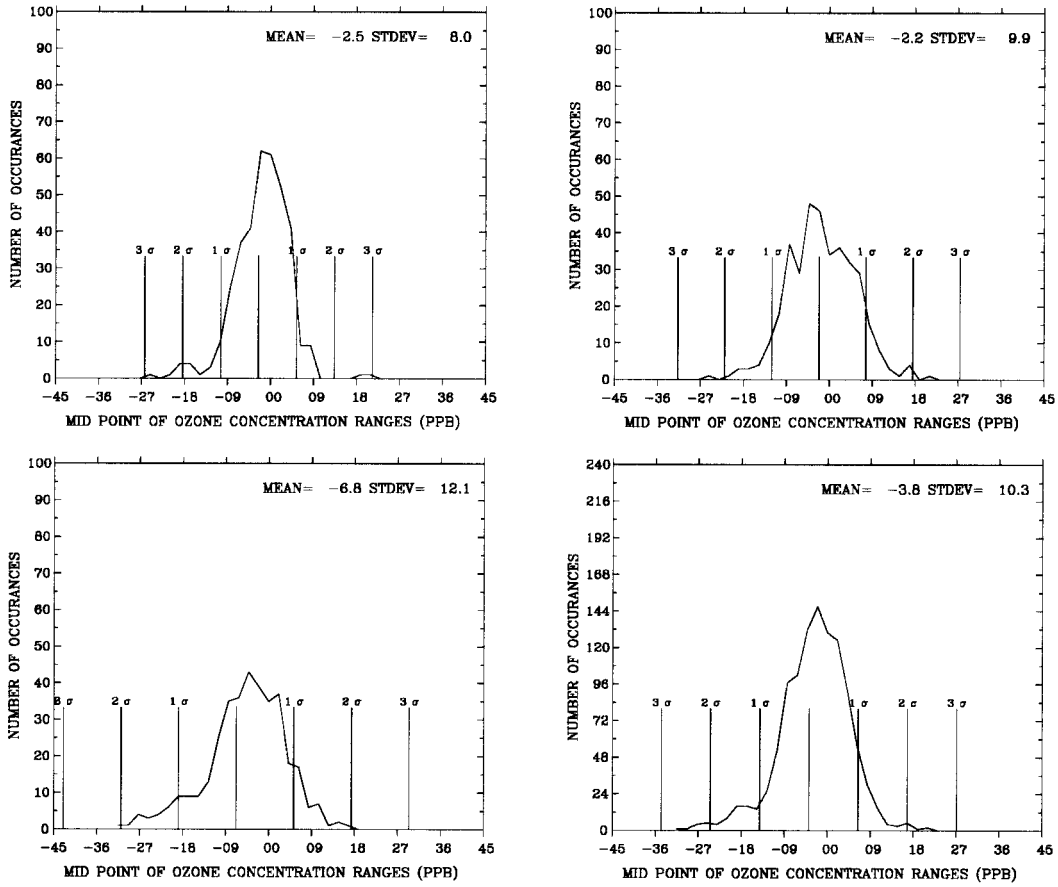

FIG. 10. Distribution of the differences between the modeled daily peak 1-h ozone values averaged over (upper left) 17–20 Jun, (upper right) 12–15 Jul, (lower left) 30 Jul–2 Aug, and (lower right) distributions in all three combined. The thin straight lines represent values that are 1, 2, and 3 standard deviations, away from the mean, respectively.

This result is consistent with the higher ventilation coefficient in the MM5/UAM-V system within the Northeast subdomain. Polluted plumes of air in urban locations are initially characterized by VOC sensitivity (NRC 1999). The relatively efficient removal of NO_x from the polluted air leads to a gradual transition to NO_x sensitive conditions. However, under near-stagnant conditions, implied by low ventilation coefficients, the removal of NO_x may not occur at a sufficient pace and, consequently, the plume of polluted air may remain under VOC-sensitive condition (NRC 1999). Larger values of ventilation coefficient are indicative of greater dilution of the polluted air and enhanced removal of NO_x, thereby leading to increased sensitivity to NO_x.

TABLE 2. Root-mean-square error (rmse, ppb), mean-square-error systematic (MSES, expressed in percent), mean-square-error unsystematic (MSEU, expressed in percent), and range of variability (expressed in percent).

Month	Rmse (ppb)	MSEU (%)	MSES (%)	Range of variability
		Northeast		
Jun	9.0	77	23	22
Jul	9.5	81	19	20
Aug	11.5	79	21	24
		Midwest		
Jun	8.1	93	7	20
Jul	10.1	99	1	22
Aug	16.4	79	21	34
		Southeast		
Jun	7.8	38	62	16
Jul	10.8	56	62	20
Aug	10.6	39	61	22

There are also some isolated pockets in the modeling domain (coastal North Carolina and South Carolina, parts of Georgia, and Alabama) where the RAMS/UAM-V system shows a smaller decrease in ozone levels from reductions in NO_x when compared with MM5/UAM-V. This result gives us an overall measure of the response of the modeling systems over the three episodes, but note that there are model-to-model differences for individual episodes. However, the common feature of each episode is the greater effect of NO_x emission reductions relative to VOC emission reductions in lowering ozone concentrations.

In the following analysis, we define the index of im-

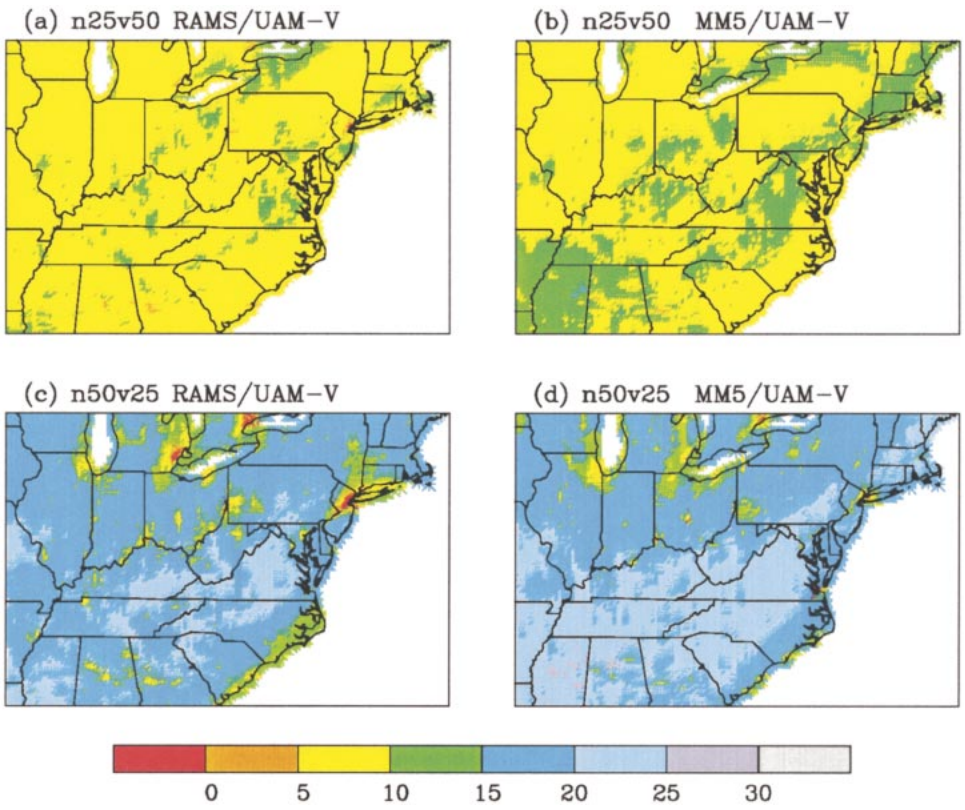

FIG. 11. Spatial distribution of the index of improvement from NO_x and VOC emission-reduction scenarios relative to the base run (n00v00), computed from episodes-averaged 1-h peak ozone.

provement relative to one of the perturbed cases. Here we use the n25v25 run as the *perturbed base* case. This is equivalent to assuming the perturbed case (n25v25) as being the base run for the other emission control scenarios, namely, n25v50 case and n50v25 case. The rationale for such a method of analysis is that, relative to the n25v25, these two perturbed runs represent equal cut in VOC and NO_x emissions, respectively. In this way, we can examine the efficacy of NO_x-focused versus VOC-focused emission reductions on improving ozone levels. The n25v50 control run is equivalent to a VOC control run that reduces anthropogenic VOC by 25% from the perturbed base case and the n50v25 case can be considered as a perturbed run that reduces anthropogenic NO_x by 25% from the perturbed base case.

Because we are interested in the region-to-region differences in the two modeling systems in addition to the episode-to-episode differences, we separated all grid cells within the UAM-V fine grid domain into different subdomain described earlier (Fig. 1). We considered all grid cells within each subdomain in this analysis. The index of improvement for NO_x controls against the index of improvement for VOC controls, that is, an equal reduction of NO_x and VOC from the base case by 25% each, computed using the episodes-average peak 1-h ozone is depicted in Fig. 12; this set of figures includes all three regions from both modeling systems. Grid cells that have a change in ozone of less than 1 ppb and those over the ocean are excluded in this plot. If the reductions in NO_x and VOC had identical effects on ozone concentrations, then all the points would lie along the dashed line (linear relation). However, as is evident from each panel in Fig. 12, the points have a greater spread along the *y* axis, indicating that the reductions in NO_x emissions lead to a much wider range of response in the ozone concentrations as compared with reductions in VOC emissions. This result is consistent with Fig. 11, which shows that both models exhibit greater sensitivity to the reductions in NO_x emissions than to VOC emissions.

The number within each quadrant of the panels in Fig. 12 denotes the percentage of the total number of grid cells that are plotted within each quadrant. Data in the upper-right quadrant reflect both NO_x-limited and VOC-limited conditions while data in the lower-left quadrant reflect the so-called ozone disbenefits due to both NO_x and VOC reduction. The lower-right quadrant has grid cells that show reduction in peak ozone level due to VOC emission reductions and increase in the peak ozone level due to NO_x emission reductions. The upper-left quadrant has grid cells, showing increase in the peak ozone level due to VOC emission reductions and reduction in peak ozone level due to NO_x emission reductions.

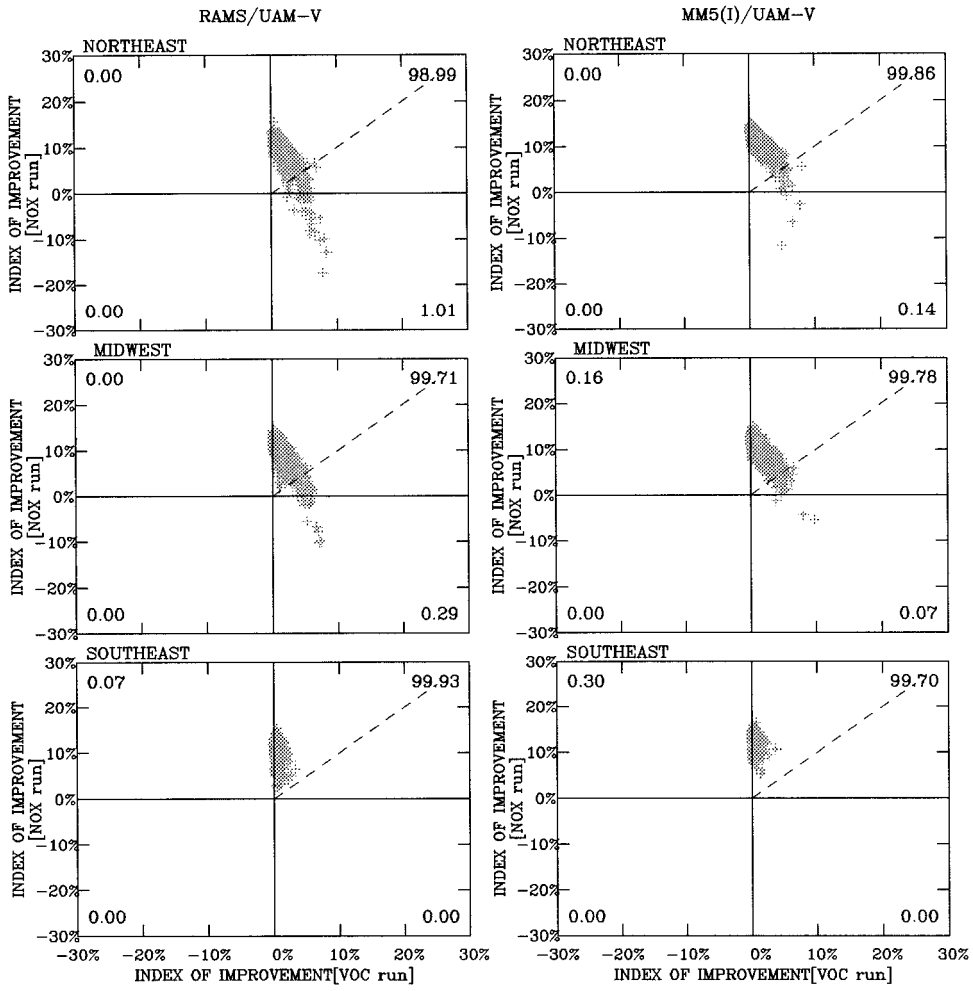

FIG. 12. The index of improvement from NO_x emission reductions plotted against the index of improvement from VOC emission reductions for episodes-averaged 1-h peak ozone from (left) RAMS/UAM-V and (right) MM5/UAM-V simulations over the (top) Northeast, (middle) Midwest, and (bottom) Southeast subdomains.

The results in Fig. 12 reveal that both modeling systems simulate slightly different responses to emission controls, even though the percentage of grid cells falling within each quadrant is comparable in both modeling systems. In each subregion, the MM5/UAM/V system shows a slightly greater effectiveness of NO_x controls than does the RAMS/UAM-V system. In the lower-right quadrant of each panel in Fig. 12, which emphasizes VOC controls, we see that there is a higher percentage of points from RAMS/UAM-V than MM5/UAM-V in the Northeast and the Southeast. Thus, the two modeling systems with different meteorological drivers provide slightly different results regarding the NO_x-sensitive and VOC-sensitive regimes at some grid cells, though at the majority of the grid cells the two modeling systems show that they are affected similarly by both NO_x and VOC reductions. However, the magnitude of ozone improvement resulting from NO_x reductions is greater than from VOC reductions. Individual episodes show similar results although the actual percentage of grid cells in each quadrant shows a variation from one episode to the other (not shown).

To evaluate the day-to-day variability in the difference in the peak ozone concentrations simulated by the two modeling systems for the base-case simulation and day-to-day variability in the difference between the efficacies of emission controls simulated by the two modeling systems, we define the metric, the coefficient of variation, as follows. For the n00v00 simulation, it is the standard deviation of the difference in the daily peak ozone concentrations simulated by the two models expressed as a percentage of the mean modeled ozone over all the days of the episodes (Fig. 13a). For the n50v25 and n25v50 simulations, it is the standard deviation of the difference in the daily index of improvement given by the two models expressed as a percentage of the mean modeled index of improvement over all the days of the episodes (Figs. 13b,c).

The coefficient of variation for the base-case simulation (Fig. 13a) over most of the domain ranges from

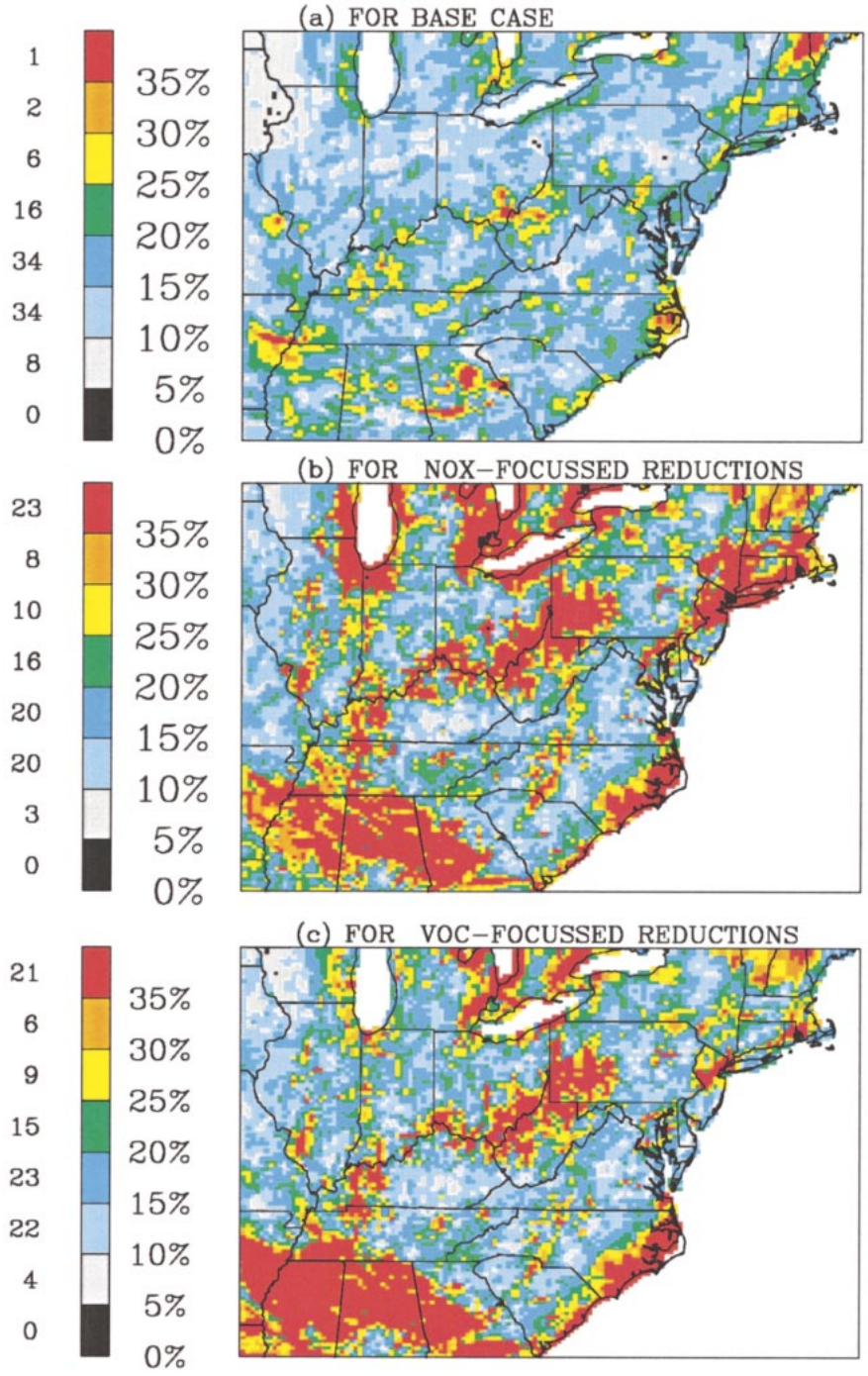

FIG. 13. The coefficient of variation for peak 1-h ozone from (a) the base case, (b) NO_x-focused emission controls, and (c) VOC-focused emission controls, over all the days of the three episodes. Numbers above the individual label bars denote the percentage of the grid cells that fall within each plotting interval.

10% to 20% of the mean predicted ozone. About 1% of all grid cells are associated with low (0%–5%) values of the coefficient of variation, and about 6% of the sites are associated with high (30%–40%) values. The northeastern urban corridor and the Lake Michigan region are seen to be associated with higher than average coefficient of variation values. Parts of coastal North Carolina, Kentucky, Ohio, and West Virginia also exhibit higher-than-average variation. On the other hand, lower-than-average values of coefficient of variations can be

seen in parts of Illinois, Iowa, and Wisconsin (Fig. 13a). For the NO_x-focused emission control (Fig. 13b) and the VOC-focused emission control (Fig. 13c), the coefficient of variation is found to be within 30% over most parts of the domain, though larger values of this metric can be seen along the Northeast urban corridor, Western Pennsylvania, the Great Lakes regions, and portions of the Southeast. A comparison of Figs. 13a–c also shows that regions such as the Ohio River valley that exhibit higher coefficient of variation for the two emission control simulations are also associated with higher coefficient of variation in the daily peak ozone levels for the base case. An additional feature of interest is the relatively larger magnitude of the coefficient of variability in the northeastern urban corridor and the regions around the Great Lakes for the NO_x-focused emission control than for the VOC-focused emission control. This result may be related to the presence of relatively higher number of NO_x-emitting sources in this region (not shown).

The results above reveal that not only is there an episode-to-episode and model-to-model uncertainty in modeling absolute levels of ozone (i.e., the base-case simulation), there is also a significant uncertainty in predicting the relative change in ozone stemming from emission reductions (i.e., the efficacy of the emission controls). Because it has been demonstrated that ozone timescales of greater than one day are most relevant to policy making (Hogrefe et al. 2000) and that emission reduction strategies are designed to affect longer-term ozone concentrations (i.e., trends), these results point the need to consider only the ozone concentrations averaged over all episodes modeled in examining the effectiveness of emission reductions from the regulatory standpoint. Further, because the effects of meteorology on ambient ozone levels must be removed to evaluate the effectiveness of ozone management efforts (NRC 1991; Cox and Chu 1993; Rao and Zurbenko 1994; Milanchus et al. 1998), ozone control strategies need to be based on their efficacy to reduce the daily maximum concentration averaged over all episode days.

4. Summary

The results from the UAM-V simulations of three high-ozone events in the summer of 1995 with meteorological inputs derived from two different meteorological models (RAMS and MM5) enable us to quantify the uncertainty associated with ozone modeling. By specifying identical emissions and initial/boundary conditions, we examined the differences in the modeled ozone concentrations arising primarily from differences in the meteorological fields. The results illustrate the model-to-model, episode-to-episode, and region-to-region variability in ozone distributions that can be expected when we use two meteorological modeling systems that yield differing meteorological fields. We find that there is an uncertainty of about 20% in simulating ozone levels for the base case. The notable result is that a major part of this variability is attributable to the unsystematic type of errors. Only the Southeast subdomain is associated with high systematic error. Berman et al (1997) showed that the uncertainties associated with estimating the temporal evolution of the mixing depth are comparable to the uncertainties in the chemical mechanisms in that model. This result is of significance, considering that, in the current case, not only are the mixing heights variable, but also other meteorological parameters are different in the two modeling systems, resulting in even greater uncertainty in modeled ozone concentrations.

Analysis of modeled and measured ozone concentrations reveals that the overall performance of both modeling systems is comparable, implying that both models are equally preferable for use in a regulatory setting. This result does not necessarily imply that the performance of the modeling systems at any specific site is always similar. As remarked earlier, region-to-region differences are evident in the modeling systems's response. However, because of episode-to-episode variability in the response of the modeling systems, a foreknowledge of the regional bias in either modeling system for an intended episodic simulation is not possible.

Two issues of interest can be identified based on the results presented in the above results: first, the presence of model-to-model differences in the simulated daily maximum ozone concentrations in each episode; and second, the region-to-region variability in ozone results of each model. The former is a reflection of the uncertainty stemming from differences in the meteorological inputs and may be viewed as a limiting factor regarding our ability to simulate absolute levels of ozone concentrations in the eastern United States. The latter issue may be of importance in designing control strategies. In particular, regions for which both models show a similar bias may lead to similar control approaches while regions for which the models show differing biases may lead to a conflicting signal for control strategies. In these situations, the eventual choice of the modeling system may play a crucial role on the choice of regulatory measures. The key findings of this study are summarized below.

- The differences in the meteorological fields obtained from the two prognostic models can lead to significant differences in the UAM-V-modeled ozone. The results reveal that ozone concentrations produced by the two modeling systems are variable even when there is a systematic difference in temperatures and mixing heights. This result is consistent with the results of Alapaty et al. (1995) in which differences in the mixing heights and temperatures in the input meteorological fields to ROM produced differences of ± 90 ppb in modeled ozone at individual grid cells. The ventilation coefficient, a meteorological parameter that includes the effects of both wind speeds and mix-

ing heights, has a greater effect on ozone variability than any of the individual meteorological variables. To examine further the role of the individual meteorological parameters in determining the uncertainty in the modeled ozone, dynamically consistent sensitivity studies must be undertaken.

- When compared with the observed ozone concentrations, neither modeling system performs significantly superiorly to the other. Investigation of the spatial distributions of the percent difference of observed and modeled ozone concentrations as well as the scatter between the two show mixed results. Statistical measures of model performance reveal that MM5/UAM-V gives slightly larger domain-wide peak ozone values than does the RAMS/UAM-V system. However, the gross absolute error shows that, on average, the performance of both models is comparable.
- The model-to-model variability in the simulated peak 1-h ozone concentrations is on the order of 20%. A large percent of the variability in the modeled ozone, particularly in the Northeast and Midwest, is composed of unsystematic errors, reflecting the inherent uncertainty associated with ozone results from these two modeling systems. In the Southeast subdomain, a larger fraction of the differences in the model results is attributed to systematic bias in the two models, which might be corrected to improve the models' performance in this region.
- As with the simulated ozone concentrations, the VOC and NO_x sensitivities are influenced by the differences in meteorological fields.
- The model-to-model differences in ozone concentrations arising from differences in the meteorological fields and chemical mechanisms are reduced when ozone levels are averaged over all the days modeled. Such longer averaging times are also most relevant to emissions-management decisions.

Acknowledgments. This work was supported by the U.S. Environmental Protection Agency under Grant R825260-01-0, the New York State Energy Research and Development Authority under Contract 6085, and EPRI under Contract WO3189-12. The authors thank G. Sistla, A. Hansen, K. Schere, and I. Zurbenko for helpful discussions. Thanks are extended to K. Zang and G. Kallos for providing the meteorological fields from MM5 and RAMS simulations, respectively. The authors also thank the two anonymous referees for their constructive comments, which have helped us to improve the clarity of presentation.

REFERENCES

Alapaty, K., D. T. Olsrud Jr., K. L. Schere, and A. F. Hanna, 1995: Sensitivity of Regional Oxidant Model predictions to prognostic and diagnostic meteorological fields. *J. Appl. Meteor.,* **34,** 1787–1795.

——, J. E. Pleim, S. Raman, D. S. Niyogi, and D. W. Byun, 1997: Simulation of atmospheric boundary layer processes using local- and nonlocal-closure schemes. *J. Appl. Meteor.,* **36,** 214–233.

Berman, S., J.-Y. Ku, J. Zhang, and S. T. Rao, 1997: Uncertainties in estimating mixing depth—comparing three mixing depth models with profiler measurements. *Atmos. Environ.,* **31,** 3023–3039.

Biswas, J., and S. T. Rao, 1999: A diagnostic assessment of UAM-V photochemical model with two meteorological drivers: RAMS 3b versus MM5. *92nd Annual Meeting of the Air and Waste Management Association,* St. Louis, MO, Air and Waste Manage. Assoc., CD-ROM. [Available from A&WMA Publications Order Dept., P.O. Box 1020, Sewickley, PA 15413.]

Chameides, W. I., R. D. Saylor, and E. B. Cowling, 1997: Ozone pollution in the rural U.S. and the new NAAQS. *Science,* **276,** 916.

Cox, W. M., and S.-H. Chu, 1993: Meteorologically adjusted ozone trends in urban areas: A probabilistic approach. *Atmos. Environ.,* **27,** 425–434.

Dudhia, J., 1993: A nonhydrostatic version of the Penn State–NCAR Mesoscale Model: Validation tests and simulation of an Atlantic cyclone and cold front. *Mon. Wea. Rev.,* **121,** 1493–1513.

EPA, 1991: Guideline for regulatory applications of the Urban Airshed Model. EPA-450/4-91-013, 89 pp. [Available from U.S. EPA, Office of Air Quality and Standards, Research Triangle Park, NC 27711.]

——, 1992: MOBIL5 workshop material report prepared by the Office of Mobile Sources, March. [Available from U.S. EPA, Office of Mobile Sources, Ann Arbor, MI 48103.]

——, 1997: National Ambient Air Quality Standards for ozone: Proposed decision. *Federal Register,* **61,** 65 717–65 750.

——, 1998: MOBILE5 vehicle emission modeling software (MOBILE5a, MOBILE5a-H, MOBILE5b). [Available online at http://www.epa.gov/oms/m5.htm.]

——, 1999: Draft report on the use of models and other analyses in attainment for the 8-hour ozone NAAQS. EPA-44/R-99 -0004, 157 pp. [Available from United States Environmental Protection Agency, Research Triangle Park, NC 27711.]

Fox, D. G., 1981: Judging air quality model performance. *Bull. Amer. Meteor. Soc.,* **62,** 599–609.

Gaza, R. S., 1998: Mesoscale meteorology and high ozone in the northeast United States. *J. Appl. Meteor.,* **37,** 961–967.

Geron, C. D., A. B. Guenther, and T. E. Pierce, 1994: An improved model for estimating emissions of volatile organic compounds from forests in the eastern United States. *J. Geophys. Res.,* **99,** 12 773–12 791.

Gery, M. W., G. Z. Whitten, and J. P. Killus, 1988: Development and testing of the CBM-IV for urban and regional modeling. EPA-600/3-88-012, 411 pp. [Available from U.S. Environmental Protection Agency, Research Triangle Park, NC 27711.]

——, ——, ——, and M. C. Dodge, 1989: A photochemical kinetics mechanism for urban and regional scale computer modeling. *J. Geophys. Res.,* **94,** 12 925–12 956.

Guenther, A. B., P. R. Zimmerman, P. C. Harley, R. K. Monson, and R. Fall, 1993: Isoprene and monoterpene emission rate variability. Model evaluations and sensitivity analyses. *J. Geophys. Res.,* **98,** 12 609–12 617.

Hogrefe, C., and S. T. Rao, 2000: Evaluating meteorological input variables for seasonal photochemical modeling on different time scales. Preprints, *11th Joint Conf. on the Applications of Air Pollution Meteorology with the A&WMA,* Long Beach, CA, Amer. Meteor. Soc., 132–137.

——, ——, L. G. Zurbenko, and P. S. Porter, 2000: Interpreting the information in ozone observations and model predictions relevant to regulatory policies in the eastern United States. *Bull. Amer. Meteor. Soc.,* **81,** 2083–2106.

Imhoff, R. E., E. M. Bailey, and S. F. Mueller, 2000: The effect of vertical diffusivity on photochemical model estimates of tropospheric ozone. Preprints, *11th Joint Conf. on the Applications of Air Pollution Meteorology with the A&WMA,* Long Beach, CA, Amer. Meteor. Soc., 116–120.

Kumar, N., and A. G. Russell, 1996: Multiscale air quality modeling

of the northeastern United States. *Atmos. Environ.,* **30,** 1099–1116.

Lagouvardos, K., G. Kallos, V. Kotroni, 1997: Modeling and analysis of ozone and its precursors in the northeast U.S.A. (atmospheric modeling simulations). Final report to Electric Power Research Institute, Palo Alto, CA, 46 pp. [Available from Office of Science and Technology, NYSDEC, Room 198, 50 Wolf Rd., Albany, NY 12233-3259.]

——, ——, ——, and S. T. Rao, 2000: An analysis of the meteorological and air quality conditions during an extreme episode over the northeastern USA. *Int. J. Environ. Pollut.,* **14,** 581–587.

Lu, C. H., and J. S. Chang, 1998: On the indicator based approach to assess ozone sensitivities and emission features. *J. Geophys. Res.,* **103,** 3453–3462.

Mathur, R., K. L. Schere, and A. Nathan, 1994: Dependencies and sensitivity of tropospheric oxidants to precursor concentrations over the Northeast United States—a model study. *J. Geophys. Res.,* **99,** 10 535–10 552.

Milanchus, M., S. T. Rao, and I. Zurbenko, 1998: Evaluating the effectiveness of ozone management efforts in the presence of meteorological variability. *J. Air Waste Manage. Assoc.,* **48,** 201–207.

Milford, J. B., A. G. Russell, and G. J. McRae, 1989: A new approach to photochemical pollution control: Implications of spatial patterns in pollution responses to reduction of nitrogen oxides and reactive organic gas emissions. *Environ. Sci. Tech.,* **23,** 1290–1301.

Morris, R. E., and T. C. Myers, 1990: User's guide to the Urban Airshed Model. User's manual for the UAM (CB-IV) modeling system. Vol. II, EPA-450/4-90-00713, 485 pp.

Nowaki, P., P. J. Samson, and S. Sillman, 1996: Sensitivity of Urban Airshed Model (UAM-IV) calculated air pollutant concentrations to the vertical diffusion parameterization during convective meteorological situations. *J. Appl. Meteor.,* **35,** 1790–1803.

NRC, 1991: Rethinking the ozone problem in urban and regional air pollution. National Academy Press, 524 pp.

——, 1999: Ozone-forming potential of reformulated gasoline. National Academy Press, 212 pp.

OTAG, 1997: Ozone transport assessment group executive report 1997. [Available online at http://www.epa.gov/ttn/otag.]

Pagnotti, V., 1987: A meso-meteorological feature associated with high ozone concentrations in the northeastern United States. *J. Air Pollut. Control Assoc.,* **37,** 720–732.

Pielke, R. A., and M. Uliasz, 1998: Use of meteorological models as input to regional air quality models—limitations and strengths. *Atmos. Environ.,* **32,** 1455–1466.

Pleim, J. E., and J. S. Chang, 1992: A non-local closure model for vertical mixing in the convective boundary layer. *Atmos. Environ.,* **26A,** 965–981.

Rao, S. T., and I. G. Zurbenko, 1994: Detecting and tracking changes in ozone air quality. *J. Air Waste Manage. Assoc.,* **44,** 1089–1092.

——, G. Sistla, V. Pagnotti, W. B. Petersen, J. S. Irwin, and D. B. Turner, 1985: Evaluation of the performance of RAM with the Regional Air Pollution Study base. *Atmos. Environ.,* **19,** 247–254.

——, I. Zurbenko, R. Neagu, S. Porter, M. Ku, and R. Henry, 1997: Space and timescales in ambient ozone data. *Bull. Amer. Meteor. Soc.,* **78,** 2153–2166.

——, and Coauthors, 2000a: An integrated modeling and observational approach for designing ozone control strategies for the eastern United States. *Air Pollution Modeling and Its Applications,* S. E. Gryning and E. Batchvarova, Eds., Vol. XIII, Kluwer Academic, 3–16.

——, J.-Y. Ku, S. Berman, K. Zhang, and H. Mao, 2000b: Summertime characteristics of the atmospheric boundary layer and relationships to ozone levels over the eastern United States. *Pure Appl. Geophys.,* in press.

Roselle, S. J., and K. L. Schere, 1995: Modeled response of photochemical oxidants to systematic reductions in anthropogenic volatile organic compound and NO_x emissions. *J. Geophys. Res.,* **100,** 22 929–22 941.

SAI, 1995: User's guide to the variable-grid Urban Airshed Model (UAM-V). SYSAPP-95/027, 128 pp.

Seaman, N. L., and S. A. Michelson, 2000: Mesoscale structure of a high-ozone episode during the 1995 NARSTO-Northeast study. *J. Appl. Meteor.,* **39,** 384–398.

Shafran, P. C., N. L. Seaman, and G. A. Gayno, 2000: Evaluation of numerical predictions of boundary layer structure during the Lake Michigan ozone study. *J. Appl. Meteor.,* **39,** 412–426.

Sillman, S., and P. J. Samson, 1995: Impact of temperature on oxidant photochemistry in urban, polluted rural and remote environments. *J. Geophys. Res.,* **100,** 14 175–14 188.

——, J. A. Logan, and S. C. Wofsy, 1990: A regional-scale model for ozone in the United States with a subgrid representation of urban and power plant plumes. *J. Geophys. Res.,* **95,** 5731–5748.

Sistla, G., N. Zhou, W. Hao, J.-Y. Ku, S. T. Rao, R. Bornstein, F. Freedman, and P. Thunis, 1996: Effects of uncertainties in meteorological inputs of Urban Airshed Model predictions and ozone control strategies. *Atmos. Environ.,* **30,** 2011–2025.

——, and Coauthors, 2001: An operational evaluation of two regional-scale ozone air quality modeling systems over the eastern United States. *Bull. Amer. Meteor. Soc.,* in press.

Tesche, T., W. P. Georgopoulos, J. H. Seinfield, F. Lurmann, and P. M. Roth, 1990: Improvements in procedures for evaluating photochemical models. Rep. A832-103, California Air Resources Board, Sacramento, CA, 200 pp.

Wilmott, C. J., 1981: On the validation of models. *Phys. Geogr.,* **2,** 184–194.

Zhang, J., and S. T. Rao, 1999: The role of vertical mixing in the temporal evolution of the ground-level ozone concentration. *J. Appl. Meteor.,* **38,** 1674–1691.

——, ——, and S. M. Daguppaty, 1998: Meteorological processes and ozone exceedances in the northeastern United States during the 12–16 July 1995 episode. *J. Appl. Meteor.,* **37,** 776–789.

Zhang, K., and S. T. Rao, 1999: Mesoscale 4DDA analyses on meteorological characteristics of high ozone episodes in 1995. 42 pp. [Available from New York State Department of Environmental Conservation, 50 Wolf Road, Albany, NY 12233.]